Rotational spectra and structures of the OC- and H_3N-HCN-HF trimers: Coaxial mixing nozzle for reactive species

T. Emilsson, T. D. Klots,[a] R. S. Ruoff,[b] and H. S. Gutowsky

Noyes Chemical Laboratory, University of Illinois, Urbana, Illinois 61801

Rotational spectra are reported for several isotopic species of the OC- and H_3N-HCN-HF heterotrimers, detected with a pulsed nozzle, Fourier transform, Balle/Flygare microwave spectrometer. Rotational constants for the main isotopic species of the OC trimer are a B_0 of 615.574 MHz and D_J of 251 Hz, and for H_3N, a symmetric top, a B_0 of 1067.161 MHz and D_J and D_{JK} of 0.40 and 63 kHz. Their structures are composites of those reported for the X-HCN and HCN-HF dimers. They are effectively axially symmetric but have some shrinkage from the distances in the dimers. The shrinkages found in r_1, the c.m. to c.m. distance for X-HCN are 0.070 and 0.098 Å for X = OC and H_3N, respectively, and in r_2 for HCN-HF, 0.033 and 0.027 Å. The ^{14}N and H-F hyperfine interactions in OC-HCN-HF are the same as those reported for the HCN-HF dimer. Detection of the X = OC and H_3N trimers out of the many species possible required care in their generation. Both were favored by the strongly bonded HCN-HF subunit. The OC-HCN-HF was further enhanced by using a high concentration of CO in the gas expansion. For H_3N-HCN-HF a coaxial mixing nozzle was developed to avoid the formation of $NH_4F(s)$. The selectivity and simplicity of the nozzle should be helpful in extending the range of species observable with pulsed nozzles.

INTRODUCTION

Rotational spectra have been observed and structures reported for a variety of hydrogen bonded and van der Waals trimers. One set of them consists of trimers containing the linear $(HCN)_2$ dimer.[1,2] They include $(HCN)_3$;[3] X-$(HCN)_2$ with X = OC, N_2, H_3N, and H_2O;[4] and $(HCN)_2$-Y with Y = HF, HCl, HCF_3, and CO_2.[5] These trimers may be viewed as composites of two dimers, the $(HCN)_2$ with X-HCN or HCN-Y. The hydrogen bond in the $(HCN)_2$ dimer is relatively strong[6] so the dimer acts largely as a subunit, enabling the trimers to be formed in readily detectable concentrations in a pulsed nozzle expansion.[7]

In the trimers characterized so far, the geometry is usually a simple overlap of that of the two dimers; for example, the linear $(HCN)_2$ plus the T-shaped HCN-CO_2 (Ref. 8) gives a T-shaped $(HCN)_2$-CO_2.[5] An exception is that the linear $(HCN)_2$ plus a quasilinear Ar-HCN (Ref. 9) gives a T-shaped trimer, with the Ar alongside a slightly perturbed $(HCN)_2$.[10] Although the geometry of the dimers is generally preserved, incorporation of them in a trimer usually produces significant shrinkage of the hydrogen bonds involved. Also, the torsional oscillations and charge distributions of the monomers are modified somewhat in the trimers compared with the dimers.

The present work extends such studies to two heterotrimers, each with three different monomers. However, two of the monomers are common to both trimers and, in fact, the trimers can be viewed as examples of X-HCN-HF, with the HCN-HF dimer as a subunit. Analyses of a variety of

dimers containing HCN have shown that HCN-HF is probably the most strongly hydrogen bonded dimer of HCN,[6] so it comes as no surprise to find it as a subunit in trimers.

The generation of H_3N-HCN-HF presented an interesting challenge. One learns in freshman chemistry that adjacent beakers of aqueous ammonia and an aqueous hydrogen halide form between them a dense white "cloud" of NH_4X solid aerosol particles. Because of this, it was necessary to modify the nozzle so that the monomers could be introduced into the jet expansion separately to avoid direct combination of NH_3 and HF to form ionic $NH_4F(s)$ and yet produce the hydrogen-bonded trimer.

An objective of this work was to determine the feasibility of generating trimers with three different components in a "linear" X-Y-Z sequence. Also, we wanted to see the extent to which the X-Y and Y-Z subunits of the trimers differed from the free X-Y and Y-Z dimers. The presentation, terminology, and analysis of these results follow those employed for the closely related X-$(HCN)_2$ and $(HCN)_2$-Y species.[4,5]

EXPERIMENT

Except for the coaxial nozzle used to form NH_3-HCN-HF, the pulsed nozzle, Fourier transform microwave spectrometer and experimental procedures were much the same as described previously.[4,5,7] In order to produce the trimers, four gases were mixed in a flow system: CO or NH_3, HCN, HF, and the carrier gas—either Ar or first-run neon (30% He, 70% Ne). The HCN and HF were 3% mixtures in He which were combined and diluted to about 0.2% with the carrier gas, usually Ar. For OC-HCN-HF the CO was added straight from the lecture bottle, and a large amount, up to 10% of the total, could be added before it reduced the

trimer signal. In Ar the backing pressure was 0.8 atm and the nozzle orifice was 0.75 mm in diameter. The [18]O labeled CO was purchased from Cambridge Isotope Laboratories. The HC[15]N was synthesized locally from KC[15]N (Cambridge) and the DF from D$_2$ and F$_2$. The [15]NH$_3$ was from Isotec, Inc.

In the experiments on H$_3$N–HCN–HF, to avoid formation of NH$_4$F(s) it was necessary to introduce HF into the jet expansion at a point where the remaining contact time between NH$_3$ and HF was too short to permit formation of larger clusters. This was accomplished by extending the idea of Hertel et al.[11] which they used to measure the ionization potential of the Na–H$_2$O dimer. For those experiments a cw oven source at 850 K generated a small beam of Na vapor which was injected at 90° into the expansion zone of a pulsed jet of argon seeded with water vapor. The expanding jet "picks up" the sodium atoms, forming a variety of sodium-water clusters.

Our requirements were less stringent in that both the injection source and the pulsed nozzle can operate at room temperature. On the other hand, Hertel's arrangement was inadequate for our purpose for several reasons: (a) the gas pressure remaining at the region where the reactants combine is too low to provide sufficient vibrational and rotational cooling of the clusters that do form. (b) The concentration of clusters formed, while adequate for mass spectrometric detection, is too low for microwave measurements. (c) The trajectories of the clusters that form are skewed relative to the pulsed nozzle axis, which results in annoying Doppler broadening and/or splitting of the lines that might be observed.

Our search for a better nozzle design was aided considerably by Legon's[12] measurement of the rotational spectrum of NH$_3$–HCl. It was accomplished with a pulsed nozzle containing solid NH$_4$Cl heated to 200 °C. Their results enabled us to observe known transitions with different arrangements for mixing the NH$_3$ and HCl. Our most successful nozzle design is shown in Fig. 1.[13] It has three parts, which form a

small, cylindrical extension to the usual pulsed valve (General Valve No. 8-1-900). The main tube (C) is a 2 cm segment of 13 gauge (2.3 mm o.d.) syringe needle attached to the bottom of the pulsed valve. A much finer injection tube (D), made from 29 gauge needle stock (0.4 mm o.d.) is inserted through a hole on the side of the main tube, positioned coaxially in it, and soldered in place. It is essential that the injection tube be placed precisely on the center of the main tube, to maintain the axial symmetry of the jet. The last part (E) is a 1 cm long adjustable brass sleeve (3.2 mm o.d.) which slips over the end of the main tube. The sleeve has a constriction and a Laval type orifice.

It is necessary that the injection tube have a very narrow bore, or a constriction at the tip, so that at least an atmosphere of pressure is required to get the desired throughput of sample. The pressure in the injection tube has to be higher than the pressure of carrier gas at the point of injection. Otherwise the sample flow stops when the solenoid valve opens.

To generate the H$_3$N–HCN–HF trimer, the HF is fed continuously through the small injection tube, while the NH$_3$ and HCN are premixed in argon (0.3% each) and pulsed through the solenoid valve. The point at which the HF is injected is critical. It is adjusted by moving the slip-fit brass sleeve relative to the main tube. The best signal was obtained when the tip of the injection tube was about 1 mm below the narrowest point in the nozzle as shown in Fig. 1. Because of the critical effect of this parameter, we plan to make it externally adjustable in future versions of the device.

It was observed that when at least one of the ingredients needed to generate a signal is introduced through the injection tube, the lines obtained are narrow and free from Doppler broadening. This is probably so because there is limited mixing of the gases and the material added through the injection tube remains stratified as a streak in the center of the jet. This behavior could be useful for the generation of molecular beams, by reducing the amount of sample lost in skimmers. After a long period of use (~ 12 hrs), a thin skirt of white solid, presumably NH$_4$F, formed at the tip of the injection tube. When used to observe transitions of species observable with the unmodified nozzle, the coaxial nozzle gives somewhat weaker signals.
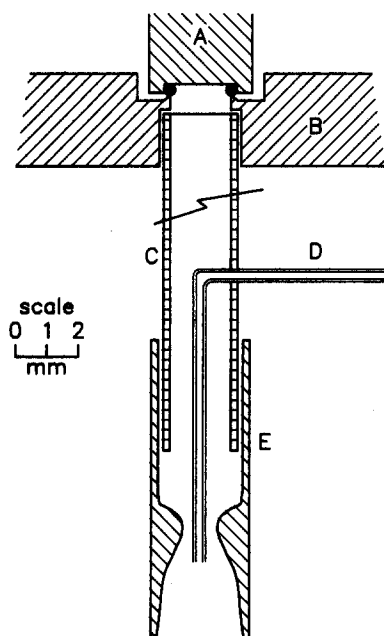

FIG. 1. Coaxial mixing nozzle developed to generate H$_3$N–HCN–HF. A and B are the plunger and bottom plate of the General Valve Co. No. 8-1-900 valve; C is the main tube of the valve extension; D is the coaxial injection tube; and E is the adjustable brass sleeve with a Laval type orifice.

RESULTS AND ANALYSIS

Transitions, identification, and rotational constants

OC-HCN-HF

The search for this trimer was based on the c.m. to c.m. distances found for the linear dimers OC–HCN[14] and HCN–HF,[15] with allowance for their probable shrinkage in the trimer. The $J = 2 \rightarrow 3$ transition in S-band was targeted because of its smaller search window. The transition was found at 3693.4 MHz and its identity verified by the hfs (hyperfine structure) which is the same as that reported for the $J = 2 \rightarrow 3$ transition of the HCN–HF dimer.[15]

The observed frequencies are given in Table I. They were fitted as described previously[5] with the Hamiltonian

$$H = H_R + H_Q + H_D, \tag{1}$$

TABLE I. Observed and fitted hyperfine components of the $J = 2 \rightarrow 3$ transition of OC–HCN–HF.[a]

Transition $F_1, F_2, F \rightarrow F'_1, F'_2, F'$	Observed (MHz)	Obs–Calc (kHz)
3,7/2,4 → 3,7/2,4	3692.0946	0.2
1,1/2,1 → 2,3/2,2	3693.1896	− 4.3
1,3/2,1 → 2,5/2,2	3693.2101	− 0.6
1,3/2,2 → 2,5/2,3	3693.2197	2.2
1,1/2,1 → 2,3/2,1	3693.2817	1.4
2,3/2,2 → 3,5/2,3	3693.3993	3.7
2,5/2,2 → 3,7/2,3	3693.4148	− 1.2
2,5/2,3 → 3,7/2,4	3693.4246	2.6
2,3/2,1 → 3,5/2,2	3693.4246	2.6
3,5/2,3 → 4,7/2,4	3693.4630	1.5
3,5/2,2 → 4,7/2,3	3693.4630	0.2
3,7/2,2 → 4,9/2,4	3693.4630	− 1.9
3,7/2,4 → 4,9/2,5	3693.4683	0.9
2,3/2,1 → 2,3/2,2	3695.1936	− 0.6
2,5/2,3 → 2,3/2,2	3695.2164	3.5
2,5/2,2 → 2,5/2,2	3695.2652	2.0
2,5/2,3 → 2,5/2,3	3695.2652	− 3.4
2,5/2,3 → 2,5/2,3	3695.3336	− 1.5

[a] The adjustable parameters determined by the fit are the line center at 3693.4160(2) MHz, $\chi_a(^{14}N) = -4.104(3)$ MHz, and $D_a(HF) = 108(3)$ kHz.

where H_R is the term for a semirigid rotor, H_Q is the ^{14}N quadrupole interaction and H_D is the H–F nuclear dipole-dipole interaction. The matrix elements of H were evaluated in the coupled basis

$$J + I_N = F_1, \quad F_1 + I_H = F_2, \quad \text{and} \quad F_2 + I_F = F. \quad (2)$$

Full matrix diagonalization was used to simulate spectra and fit the observed hfs as given in the table.

The $J = 7 \rightarrow 8$ and $8 \rightarrow 9$ transitions were also observed for the normal (16-14-1) isotopic species of OC–HCN–HF and for the $^{18}O/^{15}N$ substituted species. The $J = 10 \rightarrow 11$ and $11 \rightarrow 12$ transitions were observed for the corresponding DF species. These transitions exhibit little residual hfs and their line centers were taken to be the frequency of peak intensity. These results are given in Table II. They were fitted for each isotopic species to the linear molecule, semirigid rotor expression

$$E_J = B_0 J(J+1) - D_J J^2(J+1)^2. \quad (3)$$

TABLE III. Rotational constants[a] determined for eight isotopic species of OC–HCN–HF.

Species	HF Species		DF Species	
	B_0	D_J	B_0	D_J
16-14-1/2	615.5737(3)	251(2)	607.8051	248
18-14-1/2	589.0488	225	581.4289	219
16-15-1/2	613.9404	252	606.3068	243
18-15-1/2	587.3188	231	579.8379	222

[a] Given in MHz.

The resulting rotational and centrifugal distortion constants are listed in Table III. The standard deviations of B_0 and D_J were determined only for the normal isotopic species.

H₃N–HCN–HF

This trimer was expected to have a substantially larger B_0 than OC–HCN–HF because of the smaller NH_3 mass and relatively short NH_3 c.m. to HCN c.m. distance (3.8466 Å) reported for the H_3N–HCN dimer. Furthermore, the presence of a second ^{14}N, in the NH_3, would make the hfs more extensive. Therefore, the initial search was made for the $J = 4 \rightarrow 5$ transition, predicted to be in the 10 GHz region and found at 10 670.7 MHz. Its observation required NH_3, HCN, and HF. Also, another transition was found at 4/5 this frequency, at 8536.6 MHz, strongly indicating the sought for symmetric top. Both transitions exhibited much partially resolved hfs and evidence of both $K = 0$ and $K = \pm 1$ components.

Further support of this identification was provided by ^{15}N substitution in the HCN. This nitrogen is very close to the c.m. of the trimer so its substitution should have only a small effect upon B_0. This was verified by finding a transition 8 MHz below that at 10 670.7 MHz, needing $^{14}NH_3$, $HC^{15}N$, and HF. Ultimately both $K = 0$ and $K = \pm 1$ transition frequencies were determined for four isotopic species as listed in Table IV. There was no evidence for transitions of higher K.

The Hamiltonian of Eq. (1), with H_Q including terms for both nitrogens, was used to analyze the hfs. The analysis

TABLE II. Line centers (MHz) observed for eight isotopic species of OC–HCN–HF.

Species[a]	$J = 7 \rightarrow 8$ (HF)	$J = 8 \rightarrow 9$ (HF)	$J = 10 \rightarrow 11$ (DF)	$J = 11 \rightarrow 12$ (DF)
16-14-1/2[b]	9848.664	11 079.595	13 370.391	14 585.607
18-14-1/2	9424.319	10 602.221	12 790.270	13 952.780
16-15-1/2	9822.530	11 050.192	13 337.453	14 549.680
18-15-1/2	9396.627	10 571.063	12 755.255	13 914.579

[a] Isotopic mass numbers are given in sequence for atoms substituted in the three monomers.
[b] The fitted line center for the $J = 2 \rightarrow 3$ transition of the normal species is 3693.416 MHz.

TABLE IV. Line centers observed for four isotopic species[a] of H₃N–HCN–HF.[b]

Transition $J \rightarrow J', K$	14-14-1 (MHz)	14-15-1 (MHz)	15-14-1 (MHz)	15-15-1 (MHz)
1 → 2,0	4268.63(1)	···	···	4145.972(3)
2 → 3,0	6402.920(5)	6398.47(1)	6223.98(1)	6218.937(1)
± 1	6402.540(5)	6398.10(1)	6223.62(1)	6218.570(5)
4 → 5,0	10 671.40(5)	···	···	···
± 1	10 670.77(2)	···	···	···

[a] Isotopic mass numbers given in sequence for an atom in each monomer.
[b] The hyperfine interaction constants assumed in determining the line centers are: $\chi_a(^{14}N)$, − 3.34 and − 4.10 MHz for NH_3 and HCN, respectively; and $D_a(HF) = 109$ kHz.

is complicated by the overlapping fine structure due to the D_{JK} centrifugal distortion term which is added to Eq. (3) to give the effective energy for a prolate symmetric top,

$$E_{J,K} = E_J - D_{JK} J (J+1) K^2. \qquad (4)$$

The relatively poor S/N and dense, poorly resolved hfs for this trimer discouraged us from determining the HF interaction constants from the observed spectra. Instead, we took values for $\chi_a(^{14}N)$ and $D_a(HF)$ from the studies of the dimers[15,16] and used them to find approximate line centers for the $K = 0$ and $K = \pm 1$ components of the transition.

This was accomplished by calculating "stick" spectra of the hfs for a given $\Delta J, K$ and broadening each component with a Lorentzian line shape of appropriate width. Visual comparison of the simulations with the observed spectra proved to be adequate in determining the line centers even for the parent isotopic species which has the most congested spectrum. The entries in Table IV include estimated uncertainties which range from 1 to 50 kHz depending upon the extent of the hfs. The line centers were fitted by Eq. (4) to obtain the rotational constants B_0, D_J, and D_{JK} for the four isotopic species. The results are given in Table V.

The $K = \pm 1$ states are very high in energy to be seen at cold-beam temperatures (~ 5 K). The C rotational constant of NH$_3$, which is 198 GHz,[17] is approximately the A rotational constant of the trimer. Given the $(A-B)K^2$ dependence of the rotational energy levels the $K = \pm 1$ levels are 6.4 cm^{-1} above the $K = 0$ levels and normally would not be populated enough for observation. The detection of their transitions supports C_{3v} symmetry for the trimer by indicating that the $K = \pm 1$ states are not cooled to $K = 0$ states in the expansion because of the proton spin statistics of the NH$_3$.[16,4]

Structural analysis

Figure 2 gives a sketch for the linear OC–HCN–HF trimer. If the dimensions of the monomers are unaffected by trimer formation, I_B for the trimer is determined by r_1 and r_2, the CO to HCN and HCN to HF c.m. distances, and by θ_1, θ_2, and θ_3, the average torsional amplitudes from the a-axis for each of the three monomers. This dependence is given conveniently by the expression[4,5]

$$I_B = \sum_i m_i l_i^2 + \sum_i \frac{1}{2} \langle 1 + \cos^2 \theta_i \rangle I_i, \qquad (5)$$
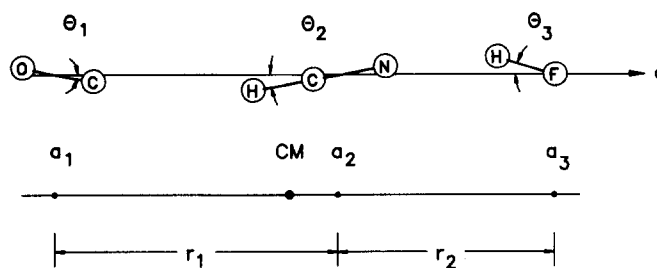

FIG. 2. Geometry of the OC–HCN–HF trimer. Atomic positions are drawn to scale. The a_i are the center of mass positions for the monomers; CM is the center of mass for the trimer and the θ_i are the average angular vibrational displacements of the monomers from the a-axis.

where m_i is the mass of the ith monomer, l_i is the distance of its c.m. to that of the trimer (Fig. 2), and I_i is I_B for the free monomers.[4,5] If θ_i and/or I_i is/are small, the torsional oscillation of that monomer has only a small effect upon the values found for r_1 and r_2. Equation (5) of course applies also to the H$_3$N–HCN–HF symmetric top.

In using Eq. (5) for the two trimers we have estimated their θ_i from values reported for the two dimers of which each is a composite. The results are summarized in Table VI. For OC–HCN–HF we have taken $\theta_1(OC)$ to be the 12° value found in OC–HCN.[14] There are two values related to $\theta_2(HCN)$, 12.5° for HCN in OC–HCN and 9.8° in HCN–HF.[15] In this case the HCN is pinned down at both ends in the trimer so we take a value of 7.5° which is less than the smallest $\theta(HCN)$ in either dimer.[3] For $\theta_3(HF)$ we use the value of 16.3° for HF in HCN–HF.[15] In H$_3$N–HCN–HF we have taken $\theta_1(NH_3)$ to be the 20.4° reported for the H$_3$N–HCN dimer.[16] For $\theta_2(HCN)$ we again have two dimer values, 9.6° in H$_3$–HCN and 9.8° in HCN–HF, and pick a value of 6.5° for the trimer. For $\theta_3(HF)$ we again use the value of 16.3° from the HCN–HF dimer.

Depending upon the data available, there are two main ways to determine r_1 and r_2. The B_0's observed for a variety of isotopic species can be fitted simultaneously to Eq. (5) with r_1^0 and r_2^0 as adjustable parameters, with allowance for the isotopic shifts in the centers of mass. The superscript identifies this type of result, which is an effective distance. In these fits the effects of the monomer bending are very small (~ 0.001 Å) for the two trimers considered here and were neglected. Alternatively, the a-coordinates of particular atoms can be determined by isotopic substitution and used to find the a_i value for that monomer's c.m. by projecting the monomer onto the a-axis with θ_i. By finding a_i(c.m.) for all three monomers, the substitution distances r_1 and r_2 are obtained by difference.

OC–HCN–HF

For this trimer the 8 B_0's in Table III were fitted simultaneously with Eq. (5), neglecting the effects of θ_i. This gave best fit values for r_1^0 and r_2^0 of 4.7679 and 3.3348 Å, respectively. The residues, not shown, are relatively large, giving an rms deviation of 115 kHz. Moreover, the calculated B_0's

TABLE V. Rotational constants determined for four isotopic species of H$_3$N–HCN–HF.

Species	B_0 (MHz)	D_J (kHz)	D_{JK} (kHz)
14-14-1	1067.161(2)	0.40(3)	63(3)
14-15-1	1066.418(5)	0.40[a]	62(3)
15-14-1	1037.336(5)	0.35[a]	60(3)
15-15-1	1036.496(1)	0.35(5)	61(1)

[a] This value was assumed for D_J to estimate B_0.

TABLE VI. Average angular displacements[a] of the monomers and substitution atomic positions in the OC– and H_3N–HCN–HF trimers.

OC–HCN–HF				H₃N–HCN–HF			
Angle	Deg.	Atom	Å	Angle	Deg.	Atom	Å
θ_1	10.85	O(1)	– 4.3518	θ_1	20.4	N(1)	– 3.7241
θ_2	7.5	N(2)	1.4898	θ_2	6.5	N(2)	0.5797
θ_3	16.2	H(3)	3.2508	θ_3	16.2	...	...

[a] Estimated from values reported for the dimers in Refs. 14–16, except for θ_1(OC) which is the projection value determined for OC–(HCN)₂ in Ref. 4.

are all too small for the DF species and too large for the HF species.

The available data also enable one to determine the *a*-coordinate of an atom in each of the parent monomers by the Kraitchman substitution method.[18] The results for ^{18}O in OC, ^{15}N in HCN, and D in HF are listed in Table VI. It is noteworthy that the mass distribution in this trimer places the nitrogen 1.5 Å from the c.m. of the trimer so the substitution position of the N should be reliable. The substitution positions a_s give in turn a_i, the c.m. positions of the monomers by the projection relation

$$a_i = a_s + d_i \cos \theta_i, \tag{6}$$

where d_i is the distance between the substituted atom and the c.m. in the *i*th free monomer. References to the structures and rotational constants of the monomers are given elsewhere.[4,5]

Application of this approach to the substitution positions in Table VI gives values of – 3.8763, 0.8982, and 4.0954 Å for a_1, a_2, and a_3. The value for a_3 is suspect because it involves D/H substitution. Therefore, we determined it independently from the results for a_1 and a_2 with the first moment condition, which gives a considerable different value of 4.2115 Å for a_3, which we adopt. Finally, the three values for a_i show by difference r_1 and r_2 to be 4.7745 and 3.3133 Å, which agree with the results for r_1^0 and r_2^0 to within 0.01 to 0.02 Å. The structural parameters determined for the OC–HCN–HF trimer are summarized in Table VII.

H_3N–HCN–HF

We used the same principles to analyze this trimer but the details differ. First the 4 B_0's in Table V were fitted simultaneously with the $\theta_i = 0$, linear version of Eq. (5), obtaining best-fit values for r_1^0 and r_2^0 of 3.7602 and 3.3082 Å. In

this case the residues are small (not given) with an rms deviation of 20 kHz. However, we have only one good substitution position, that for N(1) in the NH_3. The nitrogen in the HCN was also substituted, N(2). But it is close to the c.m. of the trimer so the determination of its position given in Table VI is unreliable.

By use of Eq. (6), the N(1) position of – 3.7241 Å yields a value of – 3.7891 for a_1. Prior experience has shown that simultaneous fitting of the B_0's for several isotopic species gives a more reliable result for the sum of r_1^0 and r_2^0 than for the individual values.[4,5] Therefore we take a_3 to be $a_1 + r_1^0 + r_2^0$ (Fig. 2), which is 3.2793 Å. In turn, application of the first moment condition to these values for a_1 and a_3 gives a_2 to be – 0.0404 Å. These results are included in Table VII along with the resulting values for r_1 and r_2 which differ by about 0.01 Å from those for r_1^0 and r_2^0.

Shrinkage

The substitution c.m. to c.m. distances in the two trimers are compared in Table VIII with those of the three dimers which they incorporate. It is seen that shrinkage of the HCN–HF distance is relatively small and very nearly the same in both trimers, averaging 0.030 Å. On the other hand, shrinkage of the OC–HCN and H_3N–HCN distances is nearly threefold greater, averaging 0.084 Å. Similar but less pronounced effects were noted for the X–(HCN)₂ and (HCN)₂–Y trimers.[4,5] Also, we point out that Δr_2^0, the shrinkage in the effective value r_2^0 for HCN–HF in OC–HCN–HF is only 0.012 Å compared with the corresponding substitution value of 0.033 Å.

Apparently a strong hydrogen bond at one end of the trimer is usually less affected than a weak one by the hydro-

TABLE VII. Structural parameters determined for the OC– and H_3N–HCN–HF trimers.

Parameter	OC–HCN–HF (Å)	H₃N–HCN–HF (Å)
r_1^0	4.7674	3.7602
r_2^0	3.3354	3.3082
a_1	– 3.8763	– 3.7891
a_2	0.8982	– 0.0404
a_3	4.2115	3.2793
r_1	4.7745	3.7487
r_2	3.3133	3.3197

TABLE VIII. Summary of substitution c.m. to c.m. distances (r_1 and r_2) in the X–HCN–HF trimers, with X = OC and H_3N, and comparison with corresponding distance in the dimers.[a,b]

X	R(X–HCN)	r_1	r_2	Δr_1	Δr_2
OC	4.8448[c]	4.7745	3.3133	0.0703	0.0330
H₃N	3.8466[d]	3.7487	3.3197	0.0979	0.0272

[a] In Å.
[b] The value of R(HCN–HF) used to determine Δr_2 is 3.3469, from Refs. 5 and 15.
[c] Reference 14.
[d] Reference 16.

gen bond at the other end. The HCN–HF bond is the strongest reported for an HCN-Y dimer.[6] Accordingly, it is changed minimally by having the relatively moderate hydrogen bonders, OC and H$_3$N at the HCN end. On the other hand, the weaker hydrogen bonds in OC–HCN and H$_3$N–HCN are strongly perturbed by having the strong HF hydrogen bonder at the other end of the HCN.

DISCUSSION

Several features of this study draw overall comment. The geometry of the H$_3$N–HCN–HF trimer is undoubtedly a symmetric top which requires that the heavy atom structure of it be effectively linear. The case for linearity of OC–HCN–HF is not as unequivocal. This trimer exhibits the rotational spectrum of a linear molecule. Moreover, its D_J value of 250 Hz is compatible with those found for the closely related X-(HCN)$_2$ trimers which appear to be linear.[4] However, the apparent absence of asymmetry doublets could be because the trimer is only slightly bent, producing nondegenerate $K = \pm 1$ states too high in energy to be visibly populated.

Also noteworthy is the virtually zero effect that the OC has on the hyperfine interactions of the HCN–HF subunit in the trimer. χ_a (^{14}N) and D_a (HF) are $-4.104(3)$ MHz and 108(3) kHz, respectively, in the trimer compared with $-4.098(4)$ MHz and 109(5) kHz in the dimer.[15] Both interactions are the same within experimental error in the two species. This may be attributed to the fact that OC is a weak hydrogen bonder, inasmuch as the OC–HCN van der Waals stretching force constant is only 3.31 N m^{-1}.[14] These observations suggest that the small value of Δr_2^0 is a better measure of the shrinkage in OC–HCN–HF than the substitution result Δr_2.

It is remarkable that each of the two trimers could be generated at sufficient concentrations for its transitions to be identified and the species characterized. For a set of three reactive monomers in the carrier gas there are 27 different trimers which can be formed, not to mention 9 dimers or the great variety of clusters containing an atom or two of the carrier gas(es). The two heterotrimers were observed in spite of this potential diversity because of strong selectivity provided by the cluster formation process in the experiments.

Presumably the trimers develop in a two-step mechanism with a dimer intermediate. Therefore, an important factor for both trimers is the exceptionally strong hydrogen bonding in the HCN–HF which favors a relatively high concentration of it in the expansion. Furthermore, the formation of OC–HCN–HF from the HCN–HF was promoted by using an exceptionally large mole fraction ($\sim 10\%$) of CO. The gas properties of CO do not differ greatly from those of the usual carrier gases so this could be done without affecting significantly the thermal characteristics of the jet expansion. The same sort of approach should enable a number of other X–HCN–HF trimers to be studied.

In the case of H$_3$N–HCN–HF the coaxial mixing nozzle was used to reduce direct contact between the NH$_3$ and HF, and prevent formation of NH$_4$F(s). This can be done in two ways—by running a mixture of NH$_3$ and HCN through the

main nozzle and adding HF with the injection tube or by using a mixture of HCN and HF and injecting NH$_3$. Both ways were tried and the first one, the injection of HF, was the most successful. The reason for this difference is a matter of conjecture because the processes in the mixing nozzle are even more complex than those in the usual nozzle.

Speculation about the difference can be based on the two-step mechanism for trimer formation. Upon injection of HF it can combine with either NH$_3$ to form the unwanted NH$_4$F(s) or with H$_3$N–HCN to form the desired H$_3$N–HCN–HF trimer. With NH$_3$ injection, the competition for it is between HF and the HCN–HF dimer. Both types of injection present a more or less equivalent opportunity for the undesired NH$_4$F(s) to be formed. However, with HF injection the desired second step is the energetically favored addition of HF to H$_3$N–HCN to give H$_3$N–HCN–HF which wins out over the weaker attraction of NH$_3$ to the HCN–HF dimer. This emphasizes the point that the mixing nozzle can be used to enhance the formation of a desired species and is not limited to avoidance of undesired species.

[1] K. Georgiou, A. C. Legon, D. J. Millen, and P. J. Mjöberg, Proc. R. Soc. London A **399**, 377 (1985).

[2] R. S. Ruoff, T. Emilsson, C. Chuang, T. D. Klots, and H. S. Gutowsky, Chem. Phys. Lett. **138**, 553 (1987). See also E. J. Goodwin and A. C. Legon, J. Chem. Phys. **82**, 4434 (1985).

[3] R. S. Ruoff, T. Emilsson, T. D. Klots, C. Chuang, and H. S. Gutowsky, Chem. Phys. **89**, 138 (1988).

[4] R. S. Ruoff, T. Emilsson, C. Chuang, T. D. Klots, and H. S. Gutowsky, Chem. Phys. (in press).

[5] R. S. Ruoff, T. Emilsson, C. Chuang, T. D. Klots, and H. S. Gutowsky, Chem. Phys. **90**, 4069 (1989).

[6] E. J. Goodwin and A. C. Legon, J. Chem. Phys. **84**, 1988 (1986), Table IX.

[7] T. J. Balle and W. H. Flygare, Rev. Sci. Instrum. **52**, 33 (1981).

[8] K. R. Leopold, G. T. Fraser, and W. Klemperer, J. Chem. Phys. **80**, 1039 (1984).

[9] T. D. Klots, C. E. Dykstra, and H. S. Gutowsky, J. Chem. Phys. **90**, 30 (1989).

[10] R. S. Ruoff, T. I. Emilsson, T. D. Klots, C. Chuang and H. S. Gutowsky, J. Chem. Phys. **88**, 1557 (1988).

[11] C. P. Schulz, R. Haugstätter, H. U. Tittes, and I. V. Hertel, Phys. Rev. Lett. **57**, 1703 (1986).

[12] E. J. Goodwin, N. W. Howard, and A. C. Legon, Chem. Phys. Lett. **131**, 319 (1986).

[13] A preliminary account of this device was given at the 43rd Symposium on Molecular Spectroscopy, Columbus, OH, 1988, Abstract TF2.

[14] E. J. Goodwin and A. C. Legon, Chem. Phys. **87**, 81 (1984).

[15] A. C. Legon, D. J. Millen, and L. C. Willoughby, Proc. R. Soc. London A **401**, 327 (1985).

[16] G. T. Fraser, K. R. Leopold, D. D. Nelson, A. Tung, and W. Klemperer, J. Chem. Phys. **80**, 3073 (1984).

[17] P. Helminger, F. C. DeLucia, and W. Gordy, J. Mol. Spectrosc. **39**, 94 (1971).

[18] W. Gordy and R. L. Cook, *Microwave Molecular Spectra* (Wiley, New York, 1984), Chap. XIII.3.